

2

AD-A237 087



OFFICE OF NAVAL RESEARCH

Grant N00014-89-J-1261

R&T Code 1113PS

Technical Report No. 5

Structure and Stability of Underpotentially Deposited Layers on Au(111) Studied
by Optical Second Harmonic Generation

by

D. A. Koos and G. L. Richmond



Administrative routing form with a checkmark and the handwritten label 'A-1'.

To be published in the Journal of Physical Chemistry

Department of Chemistry
University of Oregon
Eugene, OR 97403

May 1991

Reproduction in whole, or in part, is permitted for any purpose of the United States Government.



This document has been approved for public release and sale; its distribution is unlimited.

91 6 18 139

REPORT DOCUMENTATION PAGE				Form Approved OMB No. 0704-0188	
1a. REPORT SECURITY CLASSIFICATION UNCLASSIFIED		1b. RESTRICTIVE MARKINGS			
2a. SECURITY CLASSIFICATION AUTHORITY		3. DISTRIBUTION / AVAILABILITY OF REPORT APPROVED FOR PUBLIC RELEASE: DISTRIBUTION UNLIMITED			
2b. DECLASSIFICATION / DOWNGRADING SCHEDULE					
4. PERFORMING ORGANIZATION REPORT NUMBER(S) ONR Technical Report #5		5. MONITORING ORGANIZATION REPORT NUMBER(S)			
6a. NAME OF PERFORMING ORGANIZATION UNIVERSITY OF OREGON		6b. OFFICE SYMBOL (If applicable)	7a. NAME OF MONITORING ORGANIZATION OFFICE OF NAVAL RESEARCH CHEMISTRY PROGRAM		
6c. ADDRESS (City, State, and ZIP Code) DEPARTMENT OF CHEMISTRY UNIVERSITY OF OREGON EUGENE OR 97403		7b. ADDRESS (City, State, and ZIP Code) 800 NORTH QUINCY STREET ARLINGTON VA 22217-5000			
8a. NAME OF FUNDING / SPONSORING ORGANIZATION OFFICE OF NAVAL RESEARCH		8b. OFFICE SYMBOL (If applicable) ONR	9. PROCUREMENT INSTRUMENT IDENTIFICATION NUMBER N00014-89-J-1261		
8c. ADDRESS (City, State, and ZIP Code) 800 NORTH QUINCY STREET ARLINGTON VA 22217		10. SOURCE OF FUNDING NUMBERS			
		PROGRAM ELEMENT NO.	PROJECT NO.	TASK NO.	WORK UNIT ACCESSION NO.
11. TITLE (Include Security Classification) Structure and Stability of Underpotentially Deposited Layers on Au(111) Studied by Optical Second Harmonic Generation					
12. PERSONAL AUTHOR(S) D.A. Koos and G.L. Richmond					
13a. TYPE OF REPORT TECHNICAL		13b. TIME COVERED FROM 9/89 TO 6/91		14. DATE OF REPORT (Year, Month, Day) May 17, 1991	15. PAGE COUNT
16. SUPPLEMENTARY NOTATION submitted for publication in the Journal of Physical Chemistry					
17. COSATI CODES			18. SUBJECT TERMS (Continue on reverse if necessary and identify by block number)		
FIELD	GROUP	SUB-GROUP			
19. ABSTRACT (Continue on reverse if necessary and identify by block number) This report details changes in the second harmonic optical response from Au(111) during the underpotential deposition of Cu, Ag, Pb, and TI. The signal from Au(111) exhibits a strong anisotropy that is assigned to a coupling of the SH photons with interband transitions. Underpotential deposition is used to form overlayers of foreign metals with precise control of the surface concentration of adatoms, and the participation of the d-like electronic states in binding of metal adsorbates is evidenced in the optical response. We compare the results from the Au(111)/Cu and the Au(111)/Ag interface with those from the (111) surface of the single crystal adsorbates and find that the results are consistent with the known electronic structure of the metals and geometric structures of the overlayers. In the case of lead and thallium deposition, a strong perturbation of anisotropic second harmonic signal is observed and attributed to the inability of the large adatoms to lattice match with the substrate. The consideration of domain effects is important for the optical results to be consistent with recent structural determinations. The results are compared with related studies of Pb on Cu(111) in which interband effects also play a role. The use of second harmonic generation to monitor the stability of the overlayer in the absence of an applied field is demonstrated.					
20. DISTRIBUTION / AVAILABILITY OF ABSTRACT <input checked="" type="checkbox"/> UNCLASSIFIED/UNLIMITED <input type="checkbox"/> SAME AS RPT <input type="checkbox"/> DTIC USERS			21. ABSTRACT SECURITY CLASSIFICATION UNCLASSIFIED		
22a. NAME OF RESPONSIBLE INDIVIDUAL Professor Geraldine L. Richmond			22b. TELEPHONE (Include Area Code) (503) 346-4635		22c. OFFICE SYMBOL

Structure and Stability of Underpotentially Deposited Layers on Au(111) Studied by
Optical Second Harmonic Generation

D.A. Koos and G.L. Richmond

Department of Chemistry

University of Oregon

Eugene OR 97403

ABSTRACT:

This report details changes in the second harmonic optical response from Au(111) during the underpotential deposition of Cu, Ag, Pb, and Tl. The signal from Au(111) exhibits a strong anisotropy that is assigned to a coupling of the SH photons with interband transitions. Underpotential deposition is used to form overlayers of foreign metals with precise control of surface adatom concentration. The participation of the d-like electronic states in binding of metal adsorbates is evidenced in the optical response. We compare the results from the Au(111)/Cu and the Au(111)/Ag interface with those from the (111) surface of the single crystal adsorbates and find that the results are consistent with the known electronic structure of the metals and the geometric structures of the overlayers. In the case of lead and thallium deposition, a strong perturbation of anisotropic second harmonic signal is observed and attributed to the inability of the large adatoms to lattice match with the substrate. The consideration of domain effects is important for the optical results to be consistent with recent structural determinations. The results are compared with related studies of Pb deposition on Cu(111). The use of second harmonic generation to monitor the stability of the overlayer in the absence of an applied field is also demonstrated.

I. INTRODUCTION

Optical second harmonic generation (SHG) is a useful technique for studying adsorption processes and growth mechanisms.¹ For the study of electrochemical interfaces it is of great interest because of its unique sensitivity to interfacial properties and its experimental simplicity. In previous studies on Ag(111),² Cu(111),^{3,4} Au(111),^{5,6} and Pt(111)⁷ it has been demonstrated how the structural properties of metal electrode surfaces can be monitored by observing the variation in the SH response as the crystal is rotated azimuthally. In each case the SH response shows a three-fold symmetric anisotropy pattern that is consistent with the symmetry of a well-ordered (111) surface where the optical response is derived from at least two atomic layers.⁸ Verification of the ability to monitor the geometrical order of the surface in solution has come from recent studies comparing Ag(111)⁹ and Cu(111)¹⁰ results in ultra-high vacuum (UHV) to those obtained in solution. SHG has also been used to monitor the geometry of the interface in the presence of electrodeposited overlayers.^{2,5,11}

Recent wavelength dependent studies have shown that the SH response in general, and the rotational anisotropy in particular, is critically dependent on the detailed electronic structure of the interfacial region.^{12,13} It is crucial, therefore, to consider how the adsorption process affects the electronic structure of the interface, as well as the *geometry of the interface, when interpreting rotational anisotropy results*. This paper demonstrates in detail how the electronic properties of the metal surface can be altered by electrodeposition and how these changes can be assigned to changes in the geometrical structure of the interface. This will be demonstrated by studies of deposition on Au(111). Comparison with deposition on Cu(111) will also be made.

In addition, we demonstrate the use of SHG to monitor the stability of the UPD layer as the applied bias potential is removed. An evaluation of the stability of the deposits is valuable from a practical standpoint, as well as the suitability of a particular system for ex-situ studies (e.g. in UHV) which must be preceded by electrode emersion.

II. Theory

Treating the incident and SH EM fields classically leads to this expression for the measured SH intensity, $I(2\omega)$:¹⁴

$$I(2\omega) = (32 \pi^3 \omega^2) (A \cdot c)^{-3} \sec^2 \theta^{2\omega}_1 | e^{2\omega} \cdot \chi^{(2)} : e^\omega e^\omega |^2 I(\omega)^2 A T, \quad (1)$$

where $\theta^{2\omega}_1$ is the angle between the reflected SH beam and the surface normal.¹⁵ The intensity of the incident beam is given by $I(\omega)$, and A is the illuminated area.

The propagation vectors e^ω and $e^{2\omega}$ describe the fundamental and harmonic fields in the metal.¹⁶ We describe the surface response in the x,y,z coordinate system where the x direction lies along the $\bar{2}\bar{1}\bar{1}$ crystallographic direction and the z direction is normal to the surface (111 direction). The angles ϕ and θ_{in} describes rotation of the sample about the z axis and the angle of incidence, respectively. The angle ψ is the angle between the electric field vector of the fundamental EM field and the plane of incidence, $\psi = 0$ describing p-pol light. The angle ψ' denotes the polarization of the harmonic wave. The propagation vectors are then:

$$\begin{aligned} e^\omega_x &= \cos\psi t^p_{12} \cos\theta^\omega_2 \cos\phi + \sin\psi t^s_{12} \sin\phi \\ e^\omega_y &= \cos\psi \cos\theta^\omega_2 t^p_{12} \sin\phi - \sin\psi t^s_{12} \cos\phi \\ e^\omega_z &= \cos\psi t^p_{12} \sin\theta^\omega_2 \\ e^{2\omega}_x &= \cos\psi' \cos\theta^{2\omega}_2 (R^p_{12} - 1) \cos\phi - \sin\psi' (R^s_{12} + 1) \sin\phi \\ e^{2\omega}_y &= \cos\psi' \cos\theta^{2\omega}_2 (R^p_{12} - 1) \sin\phi - \sin\psi' (R^s_{12} + 1) \cos\phi \\ e^{2\omega}_z &= \cos\psi' (R^p_{12} + 1) \sin\theta^{2\omega}_1. \end{aligned} \quad (2)$$

The terms $t^{s,p}_{12}$ and $R^{s,p}_{12}$ are the classical Fresnel transmission coefficients at ω and the reflection coefficients at 2ω , respectively, for a wave incident on medium 2 from medium 1. The metal is characterized by a complex dielectric constant ϵ_2 .¹⁷ The complex angle between the refracted fundamental wave and the harmonic wave in the metal is denoted by θ^ω_2 ($\theta^{2\omega}_2$). For a given

susceptibility element, χ_{ijk} , a product of propagation vectors will yield a local field correction factor to the magnitude and phase of the observed response, $F_{ijk} = e^{2\omega_i} e^{\omega_j} e^{\omega_k}$. For a (111) surface, the SH response has four independent susceptibility elements, χ_{xxx} , χ_{zxx} , χ_{xzx} and χ_{zzz} .

The SH intensity can also be cast in the form:³

$$I(\phi) = | a^{(0)} + a^{(n)} \cdot f(n\phi) |^2 \quad (4)$$

where the form of $f(n\phi)$ depends upon the symmetry of the interface and the excitation and collection geometry. The isotropic and anisotropic terms, $a^{(0)}$ and $a^{(n)}$, respectively, contain the susceptibility elements, scaled by the appropriate Fresnel factors. For an interface having C_{3v} symmetry, the polarization dependence of the SH intensity follows the form:¹⁸

$$\begin{aligned} I_{p,p}(\phi) &\propto | a_{p,p}^{(0)} + a_{p,p}^{(3)} \cos(3\phi) |^2 \\ I_{s,p}(\phi) &\propto | a_{s,p}^{(0)} + a_{s,p}^{(3)} \cos(3\phi) |^2 \\ I_{p,s}(\phi) &\propto | a_{p,s}^{(3)} \sin(3\phi) |^2 \\ I_{x,s}(\phi) &\propto | a_{x,s}^{(0)} + a_{x,s}^{(3)} \cos(3\phi) |^2, \end{aligned} \quad (5)$$

where the subscripts $I_{i,j}$ introduce dependence on the polarization of the fundamental (i) and harmonic (j) beams and $x \equiv \psi = 45^\circ$. The composition of the rotational constants $a^{(n)}$ for the (111) surface are given in Table V, Ref. 18.

III. EXPERIMENTAL

The optical measurements are made in reflection using the 1064 nm fundamental beam from a 10 Hz, Q-switched, Nd:YAG as the excitation source. Details of the experimental set-up have been previously published.²

The Au(111) electrode was made from a high purity (99.999%) single-crystal rod 10 mm in diameter. The rod was oriented by x-ray diffraction and a 2.5 mm thick disc was cut to within 1° of the (111) plane. The surface was polished with successively finer grits of diamond paste (Buehler) down to $1 \mu\text{m}$. The electrode was then electrochemically polished in a cyanide bath¹⁹ and

subsequently annealed in an oxy/acetylene flame at a temperature of 650° C. Immediately following the flame treatment, the electrode was immersed in water of 18 MΩ resistivity (Barnstead Nanopure II system equipped with an organic-free cartridge) and transferred to the electrochemical cell. The Cu(111) electrode was prepared as in our previous study of Cu(111).⁴ The supporting electrolyte was 0.01 M HClO₄. The metal containing solutions were obtained by adding the appropriate amount of AgClO₄, CuSO₄, PbO, and Ti₂SO₄ to yield a 10 mM concentration of the metal ion. Doubly-distilled HClO₄ and high purity salts were obtained from Aldrich Chemical Co., Inc.

Electrochemical deposition was performed using the potentiodynamic sweep method under semi-infinite linear diffusion conditions at 25° C. Oxygen was excluded from the spectroelectrochemical cell by slowly flowing the solution (1ml/min) from a bath of electrolyte purged of O₂ using purified N₂. The triangular potential program was applied by a potentiometer (Princeton Applied Research (PAR) Model 173) equipped with a Universal Programmer and a digital coulometer (PAR Model 179). The current and charge passed were registered by an X-Y recorder (Soltec, Inc.). The sweep rate (ν) was held at either 5 or 10 mv/s.

The concentration of adatoms (Γ) at the surface of the Au(111) electrode was calculated from the charge passed in the anodic stripping of the deposit (Q_T) corrected for the surface roughness. The roughness factor of the electrode was determined from the charge passed during the formation of an anodic oxide layer (Q_o).²⁰ The surface concentration is then given as $\Gamma = Q_T \cdot 444 \times 10^{-6} / \gamma F \cdot Q_o$, where the numerical factor comes from the calculated charge for a two electron oxidative process on the gold surface and F is Faraday's constant. Electrosorption valencies (γ) of unity were assumed. The surface coverage, Θ , is defined as the concentration of adatoms at the surface divided by the maximum surface concentration (Γ_m). The latter is obtained from the concentration of gold atoms at the unreconstructed surface ($13.87 \times 10^{14} \text{ cm}^{-2}$)²¹ and the relative sizes of the atomic radii for the substrate and the adsorbate $R = R_{ad} / R_{Au}$.²²

IV. RESULTS AND DISCUSSION

A. SHG from Au(111) without adsorbates

We initially describe our results for the native Au(111) surface. The SH intensity from Au(111) biased at the potential of zero charge in 0.01 M HClO₄ as a function of the angle of rotation is shown in Figure 1. The potential of zero charge (PZC) occurs near 0.33 V vs. Ag/AgCl (sat'd KCl) for Au(111) in non-specifically adsorbing media.²³ The data for two polarization combinations is given, $I_{p,p}$ and $I_{p,s}$. The 3m symmetry of the bulk terminated (111) surface is evident in the scans. The data is well fit by Eq. 5 using the values for the rotational constants $a_{i,j}^{(n)}$ given in the caption. The 3-fold symmetry of the optical response indicates that the signal is derived from at least the top two atomic layers. We have also measured the intensities $I_{s,p}$ and $I_{x,s}$ where, neglecting bulk terms,²⁴ $I_{s,p}(\phi) \propto |F_{zxx}X_{zxx} + F_{xxx}X_{xxx} \cdot \cos(3\phi)|^2$ and $I_{x,s}(\phi) \propto |F_{xzx}X_{xzx} + F_{xxx}X_{xxx} \cdot \sin(3\phi)|^2$. We find $a_{s,p}^{(0)}/a_{s,p}^{(3)} = 0.42 e^{\pm i67^\circ}$ and $a_{x,s}^{(0)}/a_{x,s}^{(3)} = 0.416 e^{\pm i73^\circ}$ for Au(111) at the pzc. Evaluating the radiation efficiencies using Eq. 2, values of $|X_{zxx}/X_{xxx}| = 0.39$ and $|X_{xzx}/X_{xxx}| = 1.6$ are obtained from the $I_{s,p}$ and $I_{x,s}$ data, respectively.

Holding the crystal at a fixed azimuthal angle of 90°, the rotational constants $a_{i,j}^{(0)}$ and $a_{i,j}^{(3)}$ can be monitored separately as a function of the applied bias potential. In this potential region and electrolyte, only a weak adsorption of perchlorate anion takes place.²⁰ The inserts in Figure 1 show the dependence of the terms $a_{p,p}^{(0)} \propto |F_{xxx}X_{xxx} + F_{xzx}X_{xzx} + F_{zzz}X_{zzz}|$ and $a_{p,s}^{(3)} \propto |X_{xxx}|$. The arrow on the x-axis of the inserts indicates the pzc. The intensity $I_{p,p}$ shows a strong potential dependence as noted in previous studies.²⁵ No strong potential dependence is seen in the $I_{p,s}$ signal.

We are interested in monitoring $I_{p,s} \propto |X_{xxx}|^2$, the anisotropic SH response, during the underpotential deposition of different metals. We conclude that this anisotropy on Au(111) involves a coupling of the SH field with an interband transition because interband transitions are optically accessible by fields polarized in the plane of the surface (E_x and E_y) and the interband transition threshold (5d-6s) for Au(111) occurs at 2.25 eV,²⁶ energetically accessible to the SH

photons (2.34 eV). We discount the involvement of surface states in the anisotropic response at these wavelengths for several reasons. The intrinsic surface states around Γ on the (111) surface have been shown in previous studies to exhibit strong Stark shifts in the presence of an applied field.²⁷ The lack of potential dependence for χ_{xxx} in our experiments indicates that the band of partially occupied surface states is not involved in the $I_{p,s}$ signal. There is also the suggestion from other work that transitions involving the intrinsic surface states of the noble metals are induced only by photons polarized in the z direction.²⁸

B. Cyclic Voltammetry

The potentiodynamic desorption spectra for metallic monolayers of Cu, Ag, Pb, and Tl on Au(111) are shown in Figure 2. The data was collected by sweeping the applied potential positive of Nernst potential ($E_{Me/Me^{z+}}$) at a constant sweep rate and recording the generated currents. The data has been plotted as the reduced pseudo-capacitance, $C = i / \nu z$, as a function of the relative electrode potential, $E_r = E - E_{Me/Me^{z+}}$. The results are in good agreement with earlier reported spectra.²⁹ Kinetic effects were observed for the deposition of lead, with the large peak at $E_r = 230$ mV splitting into two peaks at higher scan rates. The voltammetry for copper also showed a marked dependence on scan rate. The formation of a thallium bilayer, distinguished from the bulk deposit, has been noted.³⁰ The data presented here is restricted to the monolayer region.

C. Anisotropic SH Response from Metal Overlayers

The rotational anisotropy, $I_{p,p}$, for the Au(111)/Me interface is shown in Figure 3 for Me = Cu, Ag, Tl, and Pb. The observed pattern is characterized by the ratio $a_{p,p}^{(0)}/a_{p,p}^{(3)}$ obtained from a fit of the data to Eq. 5. For comparison the values of $a_{p,p}^{(0)}/a_{p,p}^{(3)}$ obtained from Figures 1 and 3 together with the results for Ag(111) and Cu(111) are summarized in Table 1.

Monitoring the development of changes in the anisotropic response as a function of adatom coverage is accomplished by measuring the SH intensity $I_{p,s}(90^\circ)$ and the charge passed

during the potential sweep. The results for the anodic potential sweep are shown in Figure 4. Since the susceptibility χ_{xxx} does not show any strong dependence on bias potential in the voltage region scanned, changes in the optical response in Figure 4 are due solely to adsorbate induced effects.

We first discuss the results in the high coverage regime and compare the results to the optical response of the native Au, Ag, and Cu (111) surfaces. Silver or copper deposition illicit a relatively minor change in the magnitude of χ_{xxx} and the observed anisotropy. The deposition of copper (Figure 3a) causes a 23% increase in the ratio $a_{p,p}^{(0)}/a_{p,p}^{(3)}$. This is accompanied by a change in the relative phase of $a_{p,p}^{(0)}/a_{p,p}^{(3)}$, resulting in a pattern close to that observed for the Cu(111) surface (see Figure 6 below). As in the Au(111)/Cu case, Ag deposition causes a small increase in the magnitude of $a_{p,p}^{(0)}/a_{p,p}^{(3)}$ but there is no significant change in the relative phase of the components. In fact, the rotational pattern seen for the Au(111)/Ag surface, Figure 3(b), resembles that obtained from the Au(111) surface in the absence of Ag. The pattern is, however, distinctly different from the rotational anisotropy observed from Ag(111) at these wavelengths where $\arg(a_{p,p}^{(0)}/a_{p,p}^{(3)}) = 90^\circ$.²

Deposition of Pb or Tl illicit a much greater change in the ratio $|a_{p,p}^{(0)}/a_{p,p}^{(3)}|$, predominantly due to the sharp decrease in the anisotropic SH signal seen in Figure 4. The decrease in anisotropic term follows the deposition process. A minimum is reached at a coverage of $\Theta = 0.47$ for Pb and $\Theta = 0.62$ for Tl.

We offer a plausible explanation for the UPD results in terms of the size of the atoms and electronic structure of adsorbate and substrate. Previous studies indicate that Ag³¹ and Cu^{32,33} form commensurate overlayers on Au(111), whereas lead and thallium have much different electronic properties and cannot fit into the gold lattice ($R_{Pb}/R_{Au} = 1.21$ and $R_{Tl}/R_{Au} = 1.18$). Based on these previous studies and our optical data, we suggest that the ability of the Ag and Cu adatoms to lattice match with the Au(111) surface results in small changes in the interband electronic structure of the interface responsible for the observed SH anisotropy. The large lead and thallium adatoms act as defect sites in the gold lattice and cause significant changes in the

electronic wave functions at the surface, resulting in a strong dependence of the SH anisotropy on surface adatom concentration. This suggestion is supported by XPS valence band spectra of Au intermetallic compounds. The interband transition threshold is significantly shifted for amalgams of dissimilar metals.³⁴ Quite to the contrary, Au adatoms on the surface of a Cu_3Au alloy have d levels essentially degenerate with bulk Au levels.³⁵ A similar lattice matching dependent, adsorbate induced effect has been noted in the surface electronic structure of $\text{W}(100)$.³⁶

From a consideration of the substrate/adsorbate geometry, the retention of a 3-fold symmetric response from the Ag or Cu commensurate overlayer is expected. The fact that the 3-fold anisotropic response should not completely vanish for high adatom coverages of Tl or Pb as seen in Figure 3 is not as intuitive. The structures for lead and thallium UPD layers on the (111) surfaces of gold and silver have been studied by x-ray scattering.^{37,38} At monolayer coverages the data is consistent with a hexagonal close-packed overlayer, incommensurate and slightly rotated ($\sim 5^\circ$) from the substrate lattice. The long range symmetry of the interface in the presence of such an overlayer is reduced to C_1 . The form of the SH response predicted by Eq. 4 in this case has rotational amplitudes which vary as $\cos(\phi)$ and $\cos(2\phi)$, as well as $\cos(3\phi)$. Having examined combinations of p and s polarization, we find no experimental evidence for rotational amplitudes other than the 3-fold symmetric $a^{(3)}$ terms. For example, the intensity, $I_{p,s}$, at $\theta \approx 1$ for Pb and Tl shows a pattern identical to that seen in Figure 1b, although the signal level is significantly reduced. The apparent inconsistency between the x-ray scattering results and the SH data can be understood in terms of the domain structure of the overlayer on the (111) surface. It is known that two domains of the hexagonal lead overlayer exist on the $\text{Au}(111)$ surface,³⁷ rotated by angles $+\phi'$ and $-\phi'$ from the gold lattice. The coherent superposition of EM fields from two equally distributed domains will cancel any anisotropic contributions to the measured response, except the three-fold symmetric anisotropy of the substrate lattice. This effect is illustrated in Figure 5, where the primitive unit cells for the substrate and the two overlayer domains have been drawn. The C_{3v} symmetry of the substrate lattice is preserved by the coherent summation of fields from the two domains. The result depends on an equal distribution of overlayer domains. The deposition of

antimony, bismuth, or arsenic on Au(111) causes the s-polarized SH signal to decline in a manner similar to the results for lead and thallium presented here.³⁹

The behavior of the optical response in the low coverage regime needs further comment. The process of lead deposition on single crystal gold surfaces has been elucidated by an elegant set of experiments on a series of stepped surfaces by A. Hamelin and coworkers⁴⁰ together with recent structural determinations by GIXD³⁷ and STM.⁴¹ The dominant feature in the CV for Pb deposition and stripping on Au(111) is a sharp peak observed in Figure 2 at $E_p = 0.22$ V. Following this strong, sharp peak in the stripping voltammogram is a broad feature appearing ca 0.6 V that shows highly irreversible behavior. This feature is unique to the (111) surface and according to the authors of Ref. 36 is linked to terraces which are at least six atoms wide. At potentials intermediate between the main stripping peak and the highly irreversible feature another broad feature is occasionally observed. This additional feature is highly dependent upon the surface quality (preparation and orientation) and is related to reduction of Pb from step edges, correlating with the peak for Pb deposition on Au(110). From their STM work, the authors of Ref. 40 conclude that the deposition process involves initial growth at Au step edges followed by nucleation and growth of 2-D islands on Au terraces. They see no evidence of a highly irreversible process on the terraces and, in fact, conclude that the surface is void of any adsorbed species at potentials negative of $E_p = 0.6$ V. The authors do indicate that the terraces appear altered by the deposition process.

The optical data seen in Figure 4 is consistent with growth by island formation. However care must be taken in interpretation of the optical data because the decline in the anisotropy may reflect the local site symmetry of the individual atoms. That is, an individual adatom will lower the local site symmetry of the neighboring gold atoms, and this local effect may cause the decay observed in the observed anisotropy. While we cannot distinguish between these two growth mechanisms, there is important information contained in the potential dependence of the SH anisotropy. The strong dependence of the anisotropic SH signal $I_{p,s}(30^\circ)$ seen in Figure 4 occurs at low coverages and is correlated to the highly irreversible peak seen at positive potentials. As a result the SH data shows that a surface process is occurring on the (111) terraces prior to the main

deposition peak and that some surface species remains on the terraces following main desorption peak. This is in agreement with results of linear reflectance measurements,⁴² that suggest that the d-bands of the gold surface are involved in this interaction between the substrate and the adsorbate. There is a pH dependence to the hysteresis seen in the SH signal $I_{p,s}$ for deposition and stripping which follows the highly irreversible process associated with deposition on the (111) terraces.⁴³

For comparison, we have also studied the deposition of Pb on Cu(111). Figure 6 shows the SH intensity $I_{p,p}$ for Cu(111) in the absence and presence of a monolayer of Pb. In this case the lattice mismatch is large, $R_{Pb}/R_{Cu} = 1.37$. The charge passed in the formation of the Pb layer was $361 \mu\text{C}/\text{cm}^2$, corresponding to the formation of a close-packed layer with a roughness factor of 7%. The anisotropic signal declines with adsorption, as in the case of Pb and Tl on Au(111), going through a minimum before completion of monolayer. A phase change of 180° in $a_{p,p}^{(0)}/a_{p,p}^{(3)}$ takes place during the deposition. This phase shift can be seen in the rotational anisotropy (Figure 6). Using an interference technique,⁴⁴ we have determined that the phase change takes place through χ_{xxx} . As in the case of Au(111)/Pb, the anisotropic response can be understood in terms of domains of the Pb overlayer having a defined rotational angle with respect to the Cu substrate.

In the case where there is a large change in the SH anisotropy during the deposition process, monitoring the anisotropy can be used to study the stability of the deposit as conditions are changed such as removal of the applied potential. Figures 7 and 8 show the results for the anisotropic response at the Au(111)/Tl interface, $\Theta = 1 \text{ ML}$, after removal of the applied potential. The rotation anisotropy $I_{p,p}(\phi)$ is shown in Figure 7. Prior to rotation of the electrode and collection of the optical data, a monolayer of thallium was deposited on the electrode. The rotational scan was started and the applied bias potential was removed simultaneously. The rotational scan took four minutes to complete. A transformation from the SH pattern observed at the thallium covered surface to that of the native gold surface is seen to occur, indicating that the deposit is not stable in the presence of the bulk electrolyte and loss of potential control. By

monitoring the signal $I_{p,s}(t)$ the dynamics of the dissolution process can be measured. In Figure 8 the anisotropic signal $I_{p,s}(30^\circ)$ is plotted as a function of time. At time zero the Au(111) electrode is held at a potential of -0.5 V in a solution containing Tl^+ where a monolayer is formed. After 50 sec the applied potential was removed. The dissolution of the film can be modeled by including a time dependence to the adsorbate susceptibility:

$$I(t) \propto \left| 1 + 2 (b(t)/a) \cos(\alpha) (1 - \exp(-t/\tau)) + [(b(t)/a) (1 - \exp(-t/\tau))]^2 \right|, \quad (6)$$

where $b(t)$ represents the coverage (time) dependent response and α is the relative phase between the native surface response (a) and $b(t)$. The solid line in Figure 8 is a fit of the data to Eq. 6 where $b_{p,s}^{(3)} / a_{p,s}^{(3)} = -1.4 \pm 0.1$ and $\tau = 9.3 \pm 1.2$ s.

V. CONCLUSIONS

The importance of interpreting the structural information contained in the SH signal in terms of the electronic properties of the interface and possible domain effects has been emphasized in this study. In the case of Ag and Cu overlayers on Au(111) the optical signal retains a strong anisotropy showing the 3-fold symmetry of the substrate/overlayer/electrolyte region. In the case of Pb and Tl deposition, a strong perturbation of the anisotropic response is seen. This change can be tentatively assigned to the inability of the large adatoms to lattice match with the substrate, causing a substantial modification of the surface electronic structure. The involvement of the (5d-6s) interband transition in the interaction of lead and thallium adatoms with the Au(111) surface is evident in the changes in the SH anisotropy. SHG shows promise as a tool for evaluating the stability of electrodeposited overlayers.

ACKNOWLEDGEMENTS

We would like to thank P.N. Ross for the generous gift of a gold boule from which samples were fabricated. Funding for this work comes from the Office of Naval Research (N00014-89 J-1261) and the Petroleum Research Fund of the American Chemical Society (PRF-ACS 20274-AC5). The optical measurements were made at the Shared Laser Facility at the University of Oregon. G.L.R. gratefully acknowledges the Alfred P. Sloan Foundation, the Camille and Henry Dreyfus Teacher-Scholar Award, and a NSF Presidential Young Investigator Award for additional support.

References

- ¹G.L. Richmond, J.M. Robinson, V.L. Shannon, *Prog. Surf. Sci.* **1988**, *28*, 1.
- ²D.A. Koos, V.L. Shannon, and G.L. Richmond, *J. Phys. Chem.* **1990**, *94*, 2091.
- ³H.W.K. Tom and G.D. Aumiller, *Phys. Rev. B.* **1986**, *33*, 8818.
- ⁴V.L. Shannon, D.A. Koos, S.A. Kellar, P. Huifang, and G.L. Richmond, *J. Phys. Chem.* **1989**, *93*, 6434
- ⁵D.A. Koos, *J. Electrochem. Soc.* **1989**, *136*, 218C.
- ⁶A. Friedrich, B. Pettinger, D.M. Kolb, G. Lupke, R. Steinhoff, and G. Marowsky, *Chem. Phys. Lett.* **1989**, *163*, 123.
- ⁷M.L. Lynch and R.M. Corn, *J. Phys. Chem.* **1990**, *94*, 4382
- ⁸The author's of Ref. 6 observed additional rotational amplitudes in the SH response from a reconstructed Au(111) surface. Our results differ somewhat from the work of Friedrich et al. in that we do not see any evidence for a reconstructed surface. This may be due to the absence of such a reconstruction or our inability to detect it due to an equal distribution of domains of the reconstruction.
- ⁹R.A. Bradley, S. Arekat, R. Georgiadis, J.M. Robinson, S.D. Kevan, and G.L. Richmond, *Chem. Phys. Lett.* **1990**, *168*, 468.
- ¹⁰R.A. Bradley and G.L. Richmond, unpublished.
- ¹¹J. Miragliotta and T.E. Furtak, *Phys. Rev. B* **1988**, *37*, 1028.
- ¹²R. Georgiadis, G.A. Neff, and G.L. Richmond, *J. Chem. Phys.* **1990**, *42*, 4623.
- ¹³G.L. Richmond, in *Electroanalytical Chemistry*, A.J. Bard, ed. Marcel Dekker, New York, 1990, p. 87.
- ¹⁴T.F. Heinz, C.K. Chen, D. Ricard, and Y.R. Shen, *Phys. Rev. Lett.* **1982**, *48*, 478.
- ¹⁵The angle at which the SH reflection occurs is given by the expression:
- $$\theta_1^{2\omega} = \tan^{-1} \left(\sin\theta_{in} / \left((\epsilon_1(2\omega)/\epsilon_1(\omega)) - \sin^2\theta_{in} \right)^{1/2} \right),$$
- where ϵ_1 is the dielectric constant of the incident medium.

-
- ¹⁶V. Mizrahi and J.E. Sipe, J. Opt. Soc. Am. B **1988**, 5, 660.
- ¹⁷Values of $\epsilon_2(\omega) = (0.272 + 7.07i)$ and $\epsilon_2(2\omega) = (0.402 + 2.54i)$ for gold used in this work were taken from Handbook of Optical Constants of Solids, E.D. Palik, ed., Academic Press, Inc. (1985) p.294.
- ¹⁸J.E. Sipe, D.J. Moss, and H.M. van Driel, Phys. Rev. B **1987**, 35, 1129.
- ¹⁹A. Hamelin and A. Katayama, J. Electroanal. Chem. **1981**, 117, 221.
- ²⁰H. Angerstein-Kozłowska, B.E. Conway, A. Hamelin, and L. Stoicoviciu, J. Electroanal. Chem. **1987**, 228, 429.
- ²¹N.W. Ashcroft and N. D. Mermin, *Solid State Physics* (Holt, Rinehart, and Winston, Philadelphia, 1976).
- ²²C. Pariset and J.P. Chauvineau, Surf. Sci. **1978**, 78, 478.
- ²³J. Lecoeur et al. Surf. Sci. **1982**, 114, 320.
- ²⁴We have made measurements on Au(100) to investigate the possibility of higher order bulk terms contributing to the anisotropic SH signal. The results indicate that the surface response is dominant at these wavelengths and agrees with the work of others (Ref. 3).
- ²⁵P. Guyot-Sionnest and A. Tadjeddine, J. Chem. Phys. **1990**, 92, 734.
- ²⁶F. Chao, M. Costa, J. Lecoeur, and J.P. Bellier, Chem. Phys. **1990**, 141, 1627.
- ²⁷S.H. Liu, C. Hinnen, C. Nguyen Van Huong, N.R. De Tacconi, and K.M. Ho, J. Electroanal. Chem. **1984**, 176, 325.
- ²⁸M.Y. Jiang, G. Pajer, and E. Burstein, Proceed. Yamada Conf. Osaka, July 1990, Surface Science, ed. A. Yoshimori, Y. Murata, and K. Yagi (North Holland).
- ²⁹J.W. Schultze and D. Dickertmann, Surf. Sci. **1976**, 54, 489.
- ³⁰D.A. Koos and G.L. Richmond, J. Chem. Phys. **1990**, 93, 869.
- ³¹J.H. White, M.J. Albarelli, H.D. Abruna, L. Blum, O.R. Melroy, M.G. Samant, G.L. Borges, and J.G. Gordon, II, J. Phys. Chem. **1988**, 92, 4432.

-
- ³²O.R. Melroy, M.G. Samant, G.L. Borges, J.G. Gordon, J.H. White, M.J. Albarelli, M. McMillan, and H.D. Abruna, *Langmuir* **1988**, *4*, 728.
- ³³A. Tadjeddine, D. Guay, M. Ladouceur, and G. Tourillon, *Phys. Rev. Lett.* **1991**, *66*, 2235.
- ³⁴(a) T.K. Sham, M.L. Perlman, and R.E. Watson, *Phys. Rev. B* **1979**, *19*, 539; (b) G.K. Werheim, R.L. Cohen, G. Crecelius, K.W. West, and J.H. Wernick, *Phys. Rev. B* **1979**, *20*, 860.
- ³⁵W. Eberhardt, S.C. Wu, R. Garret, D. Sondericker, and F. Jona, *Phys. Rev. B* **1985**, *31*, 8285.
- ³⁶L. Richter and R. Gomer, *Phys. Rev. Lett.* **1976**, *37*, 763.
- ³⁷M.G. Samant, M.F. Toney, G.L. Borges, L. Blum, and O.R. Melroy, *J. Phys. Chem.* **1988**, *92*, 220.
- ³⁸M.F. Toney, J.G. Gordon, M.G. Samant, G.L. Borges, O.R. Melroy, L.S. Kau, and D.G. Wiesler, *Phys. Rev. B* **1990**, *42*, 5594.
- ³⁹D. Koos and G.L. Richmond, unpublished.
- ⁴⁰A. Hamelin, *J. Electroanal. Chem.* **1984**, *165*, 167.
- ⁴¹M.P. Green, K.J. Hanson, R. Carr, and I. Lindau, *J. Electrochem. Soc.* **1990**, *137*, 3493.
- ⁴²R. Adzic, E. Yeager, and B.D. Cahan, *J. Electrochem. Soc.* **1974**, *121*, 474.
- ⁴³D.A. Koos, Ph.D. Dissertation, University of Oregon, 1991.
- ⁴⁴R.K. Chang, J. Duccing, and N. Bloembergen, *Phys. Rev. Lett.* **1965**, *15*, 6.

Figure captions

Figure 1. SH intensity from Au(111) as a function of the azimuthal angle ϕ . The electrode was immersed in 0.01 M HClO₄ and biased at +0.8 V (vs. Ag/AgCl). The solid lines fits to the data using Eq. 5 in text: (a) p-pol SH, p-pol excitation, $a_{p,p}^{(0)}/a_{p,p}^{(3)} = -0.98e^{i51^\circ}$; (b) p-pol SH (x2), s-pol excitation, $a_{s,p}^{(0)}/a_{s,p}^{(3)} = 0.37e^{i119.3^\circ}$; (c) s-pol SH (x2), p-pol excitation, $a_{p,s}^{(0)} = 0$. The inserts show the dependence of $I(90^\circ)$ as a function of applied potential (vs. Ag/AgCl).

Figure 2. Potentiodynamic desorption spectra for the deposition of Cu, Ag, Pb and Tl on Au(111). The electrode was immersed in 0.01 M HClO₄, with 10 mM Me^{Z+}. Sweep rate $v = 10$ mV/s for Cu, Ag, and Tl and $v = 5$ mv/s for Pb.

Figure 3. SH intensity $I_{p,p}$ as a function of angle of rotation (ϕ) for the Au(111)/Me interface. Solid lines are fits to the data using Eq. 5. Values of the fitting parameters are listed in Table I. (a) Me = Cu, $\Theta = 0.33$; (b) Me = Ag, $\Theta = 1.0$; (c) Me = Tl, $\Theta = 0.90$; (d) Me = Pb, $\Theta = 1.0$.

Figure 4. S-pol SH intensity from Au(111) as a function of surface coverage (Θ) taken at an azimuthal angle of $\phi = 90^\circ$. Data is given for Cu (\bullet), Ag (Δ), Pb (\blacktriangle), and Tl (\circ) deposition. Lines are drawn between data points as a guide to the eye.

Figure 5. Primitive unit cells for the Au(111) substrate (solid lines, open circles) and two domains of the lead overlayer (broken lines, solid circles). One of the three mirror planes of the surface is also indicated. A rotational epitaxy angle ($\pm\phi'$) of 5° drawn and the unit cells are scaled to the experimentally determined dimensions (Ref. 37).

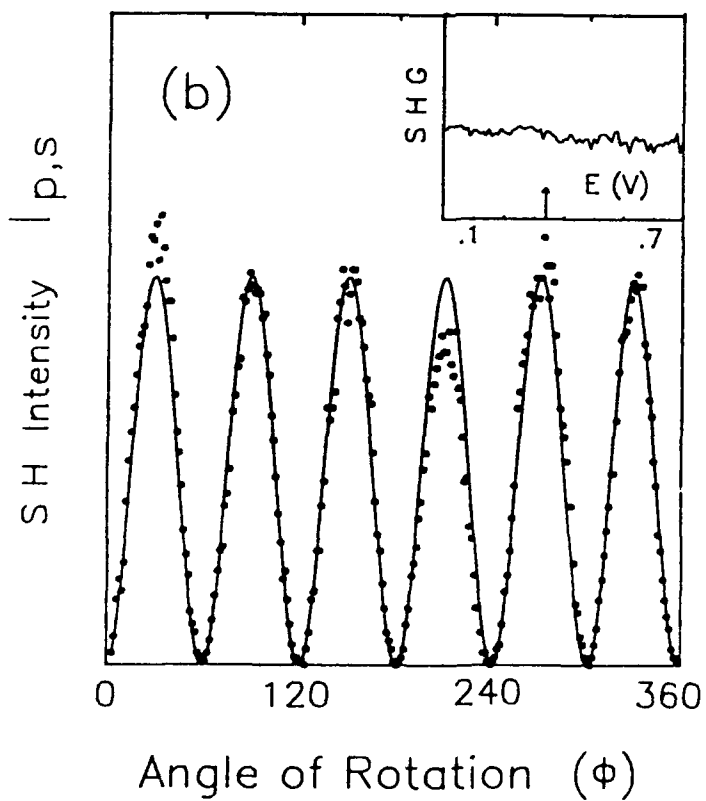
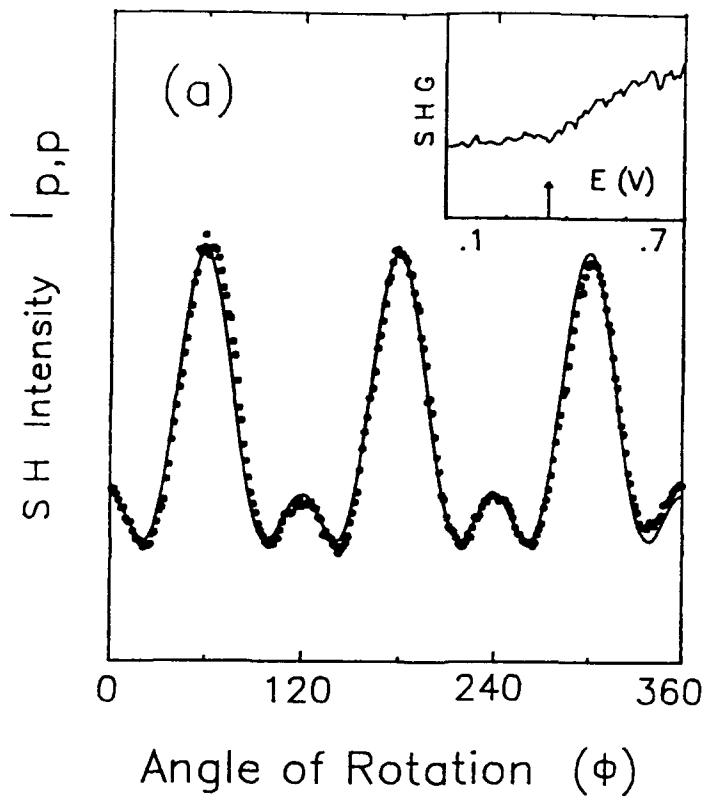
Figure 6. SH intensity $I_{p,p}$ from Cu(111) with and without a monolayer of lead as a function of the azimuthal angle ϕ . Solid lines are fits to the data with the fitting parameters listed in Table I.

Figure 7. SH intensity at the Au(111)/TI surface with no applied potential, $I_{p,p}$ as a function of ϕ . Before the rotational scan was started, $\Theta = 1$ ML. Then the applied potential was removed and the rotational scan initiated. The result is a single rotational scan, recording time of four minutes.

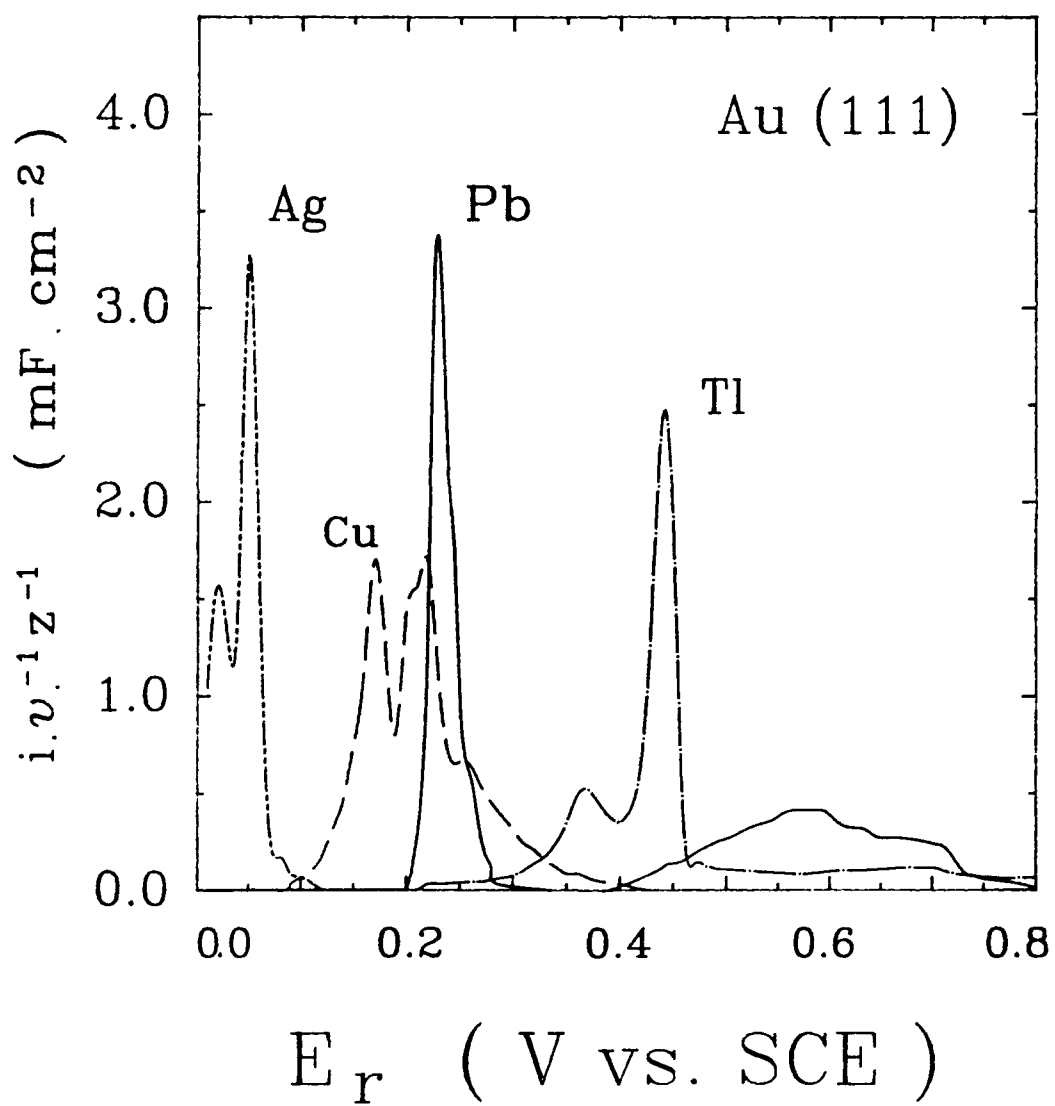
Figure 8. $I_{p,s}(30^\circ)$ as a function of time where $\Theta = 1.0$ at $t = 0$. The arrow indicates the removal of the applied potential. The solid line is a fit to Eq. 6.

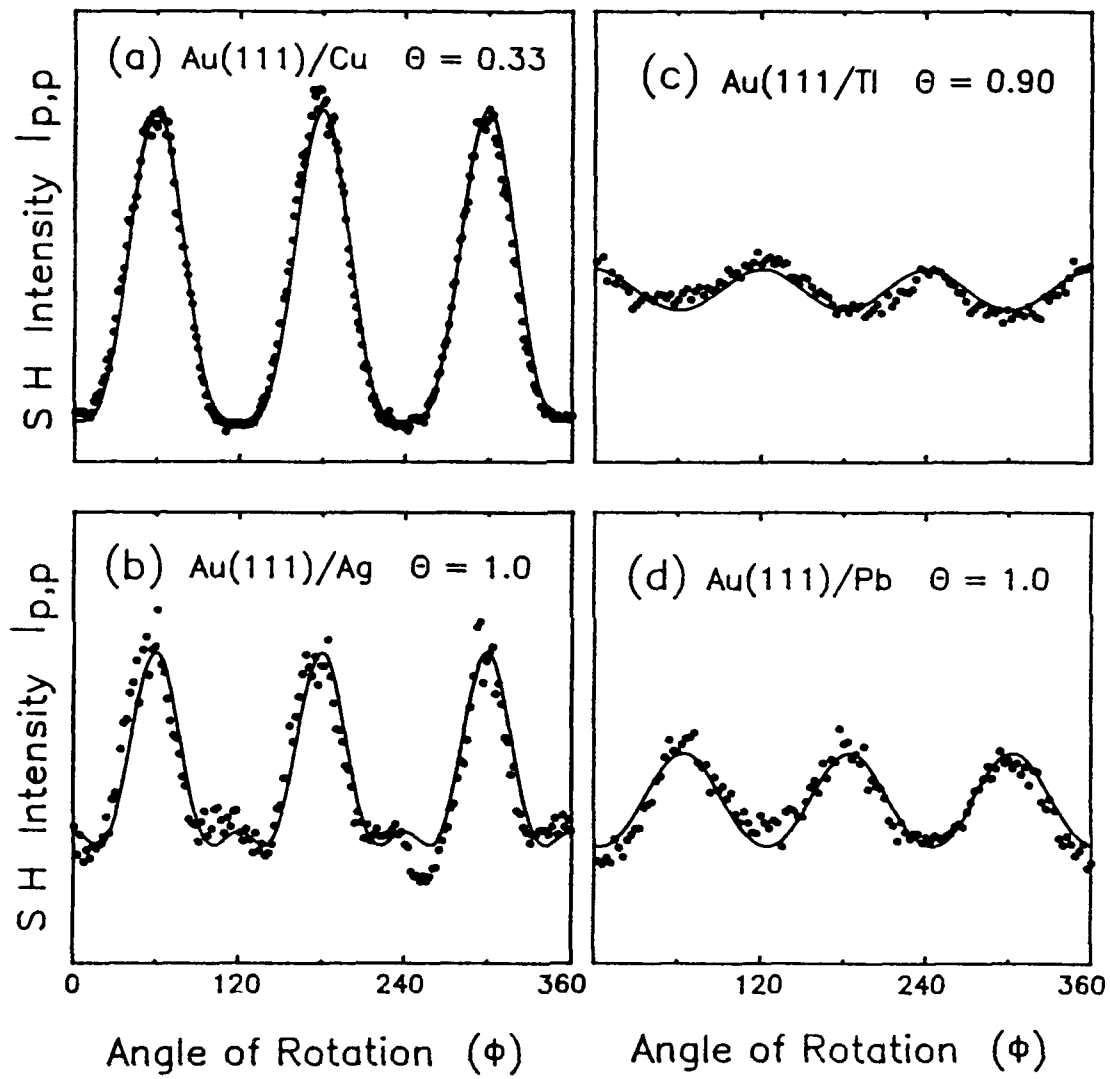
Table I. Values for the ratio of the rotational constants $a_{p,p}^{(0)}/a_{p,p}^{(3)}$ describing the $I_{p,p}$ response. Data is for native surfaces biased at the pzc and coverages approaching a monolayer, except in the case of Au(111)/Cu where $\Theta = 0.33$.

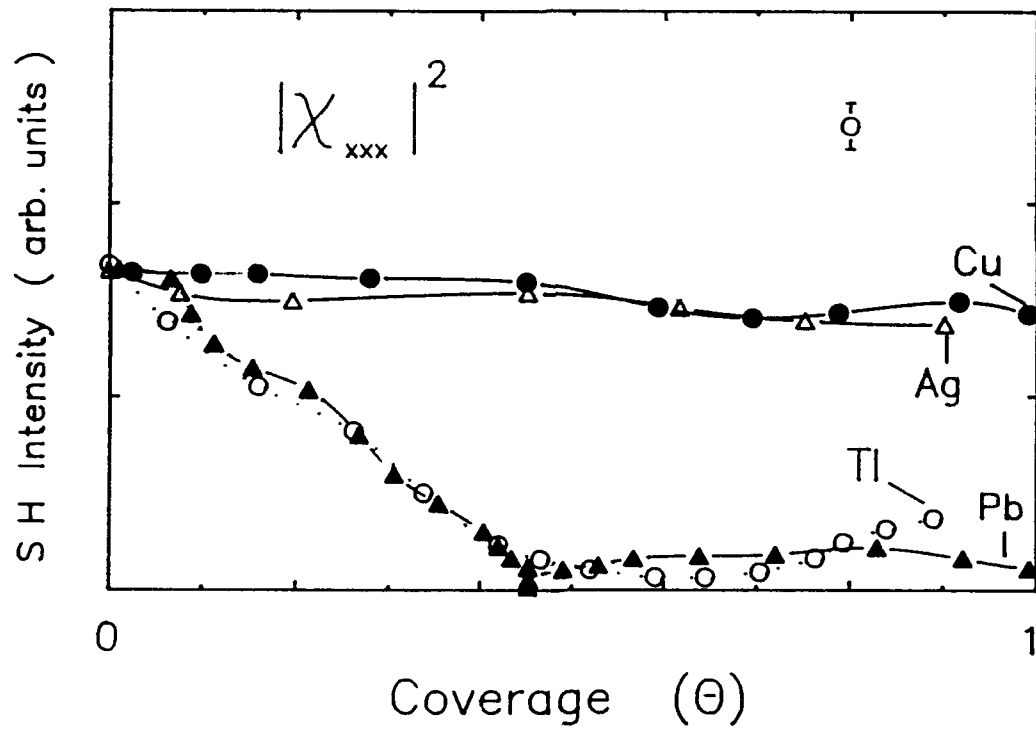
<u>Ag(111)</u>	<u>Au(111)</u>	<u>Cu(111)</u>	<u>Cu(111)/Pb</u>
$1.23 e^{\pm i87^\circ}$	$-1.02 e^{\pm i65^\circ}$	$-1.10 e^{\pm i45^\circ}$	$1.17(.06) e^{\pm i17^\circ(4)}$
<u>Au(111)/Cu</u>	<u>Au(111)/Ag</u>	<u>Au(111)/Pb</u>	<u>Au(111)/Ti</u>
$-1.26(.03) e^{\pm i35^\circ(2)}$	$-1.36(.04) e^{\pm i65^\circ(2)}$	$-3.4(.3) e^{\pm i59^\circ(3)}$	$4.5(.6) e^{\pm i74^\circ(2)}$

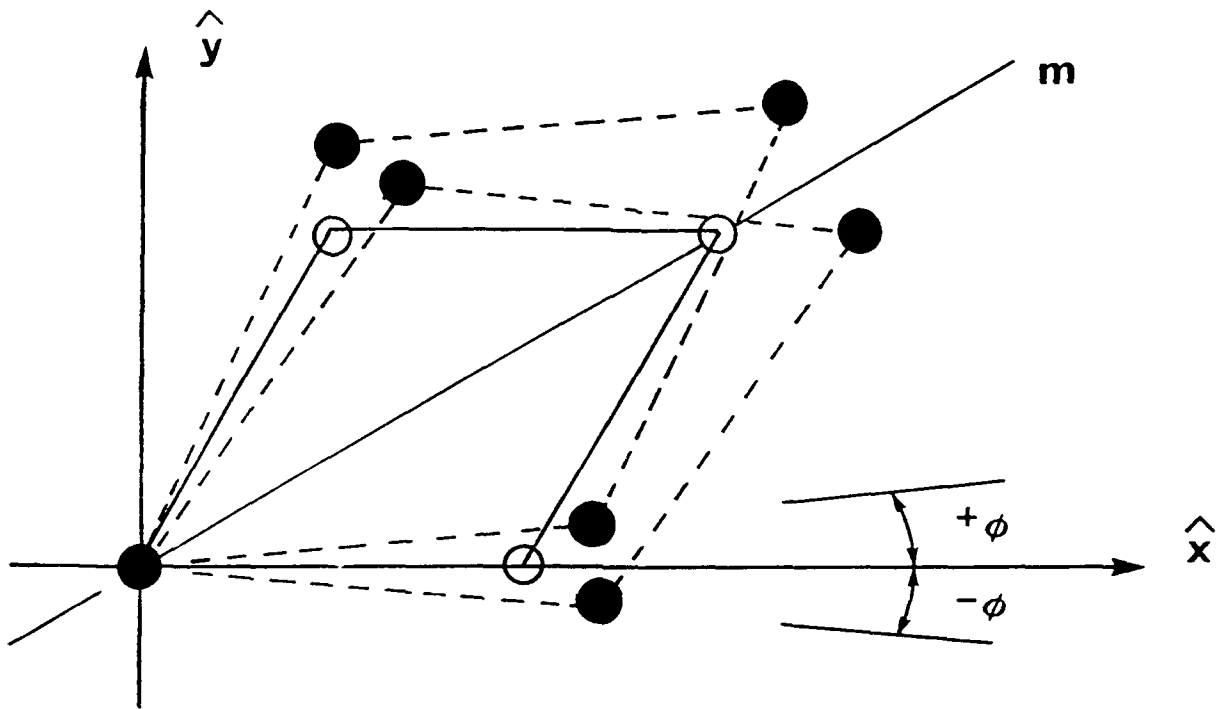


Plus there was a ?









J. Phys. Chem.
 Koos and Richmond, "Structure and Stability..."
 Figure 5

